Neuropsychiatric Disease and Treatment

Dovepress
Taylor & Francis Group

Open Access Full Text Article

ORIGINAL RESEARCH

Association Between Glymphatic Dysfunction and Anxiety in Parkinson's Disease: Insights from DTI-ALPS and Choroid Plexus Volume

Lu Sa[1], Shan Li[2], Linyu Chen[3], Jin Wang[4], Yijin Wang[1], Changxin Cheng[1], Changyuan Xin[1], Shuni Zhang[1], Fan Ding[1], Bo Wang[1]

[1]Department of MRI, the First People's Hospital of Yunnan Province, the Affiliated Hospital of Kunming University of Science and Technology, Kunming, Yunnan, 650032, People's Republic of China; [2]Department of Neurology, the First People's Hospital of Yunnan Province, the Affiliated Hospital of Kunming University of Science and Technology, Kunming, Yunnan, 650032, People's Republic of China; [3]Department of Medical Imaging, the Third People's Hospital of Honghe State, Gejiu, Yunnan, 661000, People's Republic of China; [4]Department of Medical Imaging, Southern Central Hospital of Yunnan Province (The First People's Hospital of Honghe State), Mengzi, Yunnan, 661100, People's Republic of China

Correspondence: Bo Wang, Department of MRI, the First People's Hospital of Yunnan Province, the Affiliated Hospital of Kunming University of Science and Technology, Kunming, Yunnan, 650032, People's Republic of China, Email wb13888564672@163.com

Purpose: To explore glymphatic system function in Parkinson's disease (PD) patients with anxiety using multimodal imaging: diffusion tensor image analysis along the perivascular space (DTI-ALPS), enlarged perivascular space (EPVS) number, and choroid plexus volume (CPV).

Patients and Methods: In this prospective observational study, 64 PD patients (34 with anxiety [PD-A] and 30 without anxiety [PD-NA]) and 42 healthy controls (HC) were recruited. All participants underwent clinical assessments for anxiety, depression, cognition, and motor symptoms. DTI-ALPS index, EPVS number, and CPV were compared among the three groups, and a composite model integrating these multimodal metrics was developed.Additionally,a partial correlation analysis was conducted to investigate the relationship between the above three imaging indicators and clinical characteristics in PD-A.

Results: Compared to the PD-NA, DTI-ALPS$_r$ (P =0.047) and DTI-ALPS$_b$ (P =0.01)decreased, and CPV$_l$ (P =0.046) increased in PD-A group. DTI-ALPS index was negatively correlated with CPV in PD patients.Based on receiver operating curve (ROC) analysis, the Top Single-Markers model demonstrated superior efficacy in discriminating PD from HC (AUC =0.847). Furthermore, a composite model showed predictive value for anxiety in PD (AUC =0.748). After controlling for age, gender, and education, CPV was correlated positively with Hamilton Anxiety Rating Scale (HAM-A) (r =0.657, P =0.031) and Non-Motor Symptom Scale(NMSS) (r =0.617, P =0.041).Standardized CPV was correlated negatively with Montreal Cognitive Assessment (MoCA) (r =−0.640, P =0.034) and Unified Parkinson's Disease Rating Scale III (UPDRS III) (r =0.659, P =0.03).

Conclusion: PD patients exhibit cerebral glymphatic dysfunction, which is more severe in those with anxiety. Increased CPV is associated with anxiety, depression, and cognitive decline in PD-A patients. Combining multimodal MRI metrics shows potential clinical utility for evaluating glymphatic function.

Trial registration number: NCT06858176

Keywords: glymphatic system, diffusion tensor image analysis along the perivascular space, choroid plexus volume, enlarged perivascular space, anxiety, parkinson's disease

Introduction

Parkinson's disease (PD) is the second most common neurodegenerative disease, affecting millions of people each year, and its incidence and prevalence are projected to rise with population aging.[1] The pathology of PD is characterized by degeneration of dopaminergic neurons and the accumulation of misfolded α-synuclein (α-syn).[2] The clinical features of PD encompass both motor and non-motor symptoms.[3] Motor symptoms include static tremor, bradykinesia and gait irregularities, while non-motor symptoms involve anxiety, depression, cognitive impairments, sleep disturbances, and

https://doi.org/10.2147/NDT.S568398
Received: 17 September 2025
Accepted: 16 January 2026
Published: 27 January 2026

olfactory impairment.[4–6] Previous research has predominantly focused on motor symptoms due to their more distinct clinical presentation, whereas non-motor symptoms have received comparatively less attention.[7] In fact, non-motor symptoms are highly prevalent in PD and can occur at any disease stage, even preceding motor symptom onset.[8] Anxiety affects approximately one-quarter of PD patients but is often overlooked.[4,9] Furthermore, anxiety aggravates motor symptoms in PD,[10] such as gait disturbances, which significantly impair the quality of life for sufferers and impose a substantial burden on families and society. Therefore, an awareness of anxiety in PD is crucial for prognostic assessment and personalized treatment planning.

Emerging evidence has identified a cerebral waste clearance network in human neuroanatomy, termed the glymphatic system, which consists of a cerebral glymphatic system and meningeal lymphatic vessels.[11–13] Its main function is to eliminate abnormally accumulated proteins, such as α-syn, β-amyloid, and tau proteins, which have been demonstrated to be intimately linked to neurodegenerative disorders, such as Alzheimer's disease (AD) and PD.[14–16]Currently,evaluating cerebral glymphatic function remains a major focus of research. Three common non-invasive imaging approaches are widely used: first, the DTI-ALPS index provides an indirect index of perivascular diffusivity that may be associated with glymphatic impairment, which has excellent reproducibility[17,18] and has been widely used in a range of neurologic disorders, including AD,[19] PD,[20] and epilepsy.[21] Second, the perivascular space (PVS) constitutes a crucial component of the glymphatic system. EPVS are thought to result from impaired clearance of metabolic wastes. Consequently, EPVS burden has been proposed as a potential marker of glymphatic dysfunction in previous studies.[22,23] Third, the choroid plexus (CP) is highly associated with the glymphatic system.[24] It is responsible for the production and secretion of cerebrospinal fluid(CSF), which is essential for the removal of brain wastes. Structural or functional abnormalities of the CP may disrupt cerebral homeostasis and contribute to degenerative changes in the brain.[25]

However, research on the relationship between glymphatic dysfunction and anxiety remains limited.Existing studies in this area have predominantly utilized animal models,[26,27] with scarce human research available.The underlying pathophysiology remains unclear, but it may share common mechanisms with depression,[28] which may involve AQP-4 dysfunction,[29] astrocyte impairment, and neuroinflammation.[30] Currently, there is a lack of integrated multimodal neuroimaging biomarkers to investigate this association in greater depth. Therefore, our study focusing on PD patients with anxiety aims to bridge this gap.

The study aimed to address this gap by comprehensively evaluating the brain glymphatic function in PD anxiety subtypes using a multimodal imaging approach combining the DTI-ALPS index, EPVS number, and CPV. We hypothesize that PD patients with anxiety would exhibit more severe glymphatic dysfunction, characterized by a reduced ALPS index and increased CPV, compared to those without anxiety. Additionally, we analyzed the association between the above three imaging indexes and the clinical measures (including anxiety, depression and cognition, etc.) in PD patients with anxiety.

Material and Methods

Participants

The sample size was estimated using G*Power software (version 3.1, http://www.gpower.hhu.de/).Parameters were set as follows: significance level (α) = 0.05, statistical power (1-β) = 0.8, and effect size f = 0.3 (representing a medium effect based on Cohen's conventions).[31] The final enrollment of 106 participants yields a statistical power of ~0.8 (0.785) for this study. A total of 64 PD patients and 42 healthy volunteers (HC) were recruited from the First People's Hospital of Yunnan Province between February 2024 and July 2025. The HC group was matched to the PD patients for gender and age. The severity of anxiety was evaluated according to the HAM-A, and PD patients were divided into the PD-A group (≥14 points) and the PD-NA group (<14 points). Each PD patient was diagnosed according to clinical diagnostic criteria for PD established by the International Parkinson's and Movement Disorders Society (MDS). The exclusion criteria were as follows: suffering from: (1) serious cognitive disorder that can not finish whole exam scales; (2) diseases that may affect glymphatic function, such as AD, diabetes, as well as hypertension, etc; (3) any neurologic-related diseases, including central nervous system infection, neurologic surgery, cerebrovascular disease, brain tumors (4) Parkinsonian syndrome, such as vascular Parkinson's syndrome and pharmacological Parkinson's syndrome; (5) Parkinsonian

superimposed syndrome; (6) Periventricular hyperintensity or deep white matter hyperintensity with a Fazekas score of 3; (7) contraindications to MRI examination (eg, cardiac stents or claustrophobia); (8) left-handedness. The study protocol was approved by the Clinical Research Ethics Committee of the First People's Hospital of Yunnan Province (Approval No.: KHLL2025-KY049) and was conducted in accordance with the ethical principles of the Declaration of Helsinki. All participants provided written informed permission.

Clinical Information Collection and Assessment

Basic information including age, gender, education, body mass index (BMI), disease duration, onset-age, dose of medication administered (levodopa equivalent daily dose, LEDD) and homocysteine (Hcy) was collected. All PD patients withheld anti-parkinsonian medication for at least 12 hours prior to clinical assessment and were professionally evaluated by two neurologists who were unaware of the clinical data of all subjects. The clinical assessments included the following: (1) Anxiety severity was quantified using the HAM-A. Based on the standard criteria, patients with a score of 14 and above were considered to have an anxiety. The corresponding subscores for the psychogenic anxiety factor and the somatic anxiety factor were also calculated. (2) Depression was measured by Hamilton Depression Scale (HAM-D). (3) Cognitive performance was rated with the Montreal Cognitive Assessment (MoCA) scale. (4) Quality of life measured with the 39-item Parkinson's Disease Questionnaire (PDQ-39) covering the past month.(5) Non-motor symptoms assessed using the Non-Motor Symptom Scale (NMSS) for severity and frequency over the past month.(6) Disease progression of PD was staged according to the Hoehn and Yahr classification system (H&Y). (7) Unified Parkinson's Disease Rating Scale I–III (UPDRSI, II and III) were used to assess the degree of mental activity and affective disorders, daily living activities and motor function, respectively.

MRI Image Acquisition

All scans were performed on a 3.0 T MRI system (MAGNETOM Prisma, Siemens Healthcare, Erlangen, Germany) with a 64-channel head coil. The MRI scans consisted of fast spin-echo (FSE) T2-weighted sequence, T2-weighted fluid attenuation inversion recovery (T2-FLAIR) sequence, diffusion-tensor (DTI) sequence, and high-resolution 3D sagittal magnetization-prepared rapid acquisition gradient echo (MPRAGE) T1-weighted sequence.The scanning parameters were as follows: T2WI: repetition time (TR) =4000 ms, echo time (TE) = 103 ms, field of view (FOV) = 230×230 mm^2, slice thickness = 6 mm; T2-FLAIR: TR = 8000 ms, TE = 95 ms, FOV = 230×230 mm^2, slice thickness = 6 mm, matrix = 320 × 227; DTI: TR = 4600 ms, TE = 88 ms, FOV = 256×256 mm^2, matrix = 128 × 128, slice thickness = 2 mm, voxel size = 2.0 × 2.0×2.0 mm, number of direction = 64, b value = 1000 s/mm^2, b 0 value = 0 s/mm^2. MPRAGE: TR = 1800 ms, TE = 2.26 ms, flip angle = 8°, FOV = 256×256 mm^2, matrix size = 256 × 256, slice thickness = 1 mm, voxel size = 1.0 × 1.0×1.0 mm. MRI scanning was conducted after patients had withheld anti-parkinsonian medication for at least 12 hours.

DTI-ALPS Processing

DTI-ALPS data were processed by 2 radiologists who were unaware of the clinical data. First, the raw files in DICOM format for DTI sequences were converted to the Neuroimaging Information Technology Initiative (NIFTI) file format using the MRIcroGL software (version 20-July-2022)(NITRC: MRIcroGL: Tool/Resource Info) to ensure compatibility and standardization across the data set. Then, geometric distortions were corrected using the "eddy" tool in FSL (http://www.fmrib.ox.ac.uk/FSL/). To align the adjusted diffusion gradients with the corrected images, the "rotate" function was applied. Subsequently, tensor reconstruction was performed via the "dtifit" command to create color-coded fractional anisotropy (Color FA) maps.Using ITK-SNAP (version3.8) (http://itksnap.org) draw regions of interest (ROIs), two radiologists drew regions of interest (ROIs) on the color-coded FA maps, avoiding areas of white matter hyperintensity as much as possible. Spherical ROIs with a diameter of 5 mm were placed at the level of the lateral ventricle body, focusing on areas associated with projection and association fibers, as showing Figure 1A. These ROIs were specifically aligned to capture diffusivity along the x-axis (parallel to the perivascular space) as well as the y- and z-axes (orthogonal to the perivascular space). With the ROIs confirmed, diffusivity values were calculated in the x, y, and z directions. The x-axis diffusivity represented water movement along the perivascular space, while the y- and z-axes captured diffusion in orthogonal directions. Subsequently, the left (DTI-$ALPS_l$),right (DTI-$ALPS_r$) and bilateral (DTI-$ALPS_b$) index were calculated using the following formula:

DTI-ALPS index = mean (Dx,proj, Dx,assoc)/mean (Dy,proj, Dz,assoc).

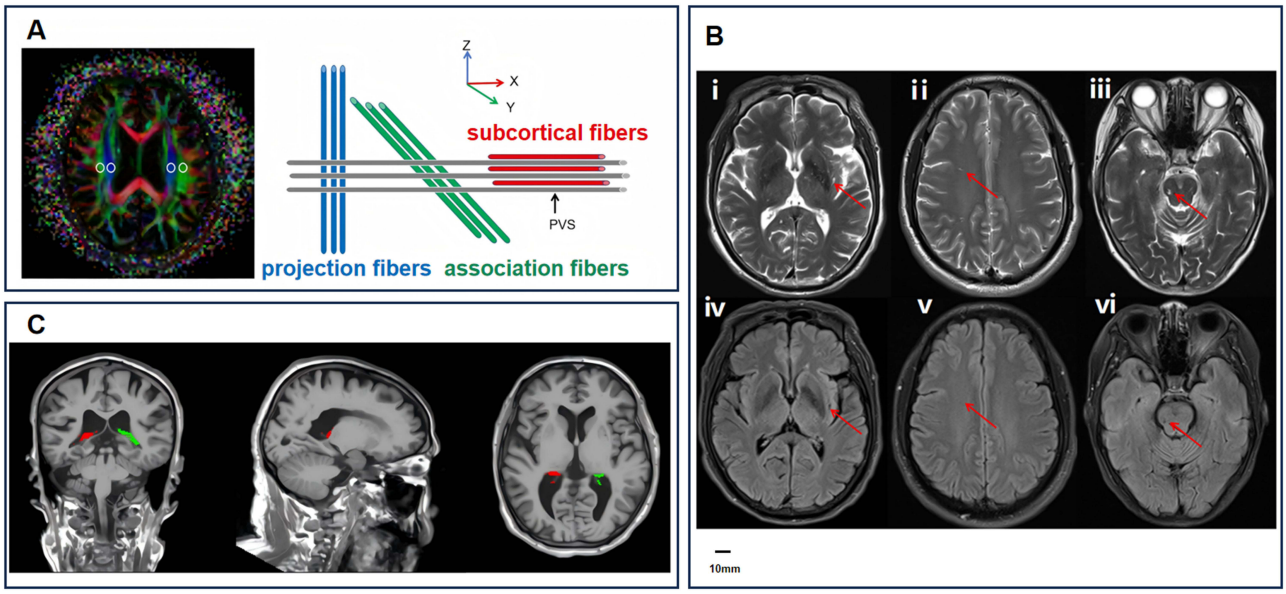

Figure 1 Schematic diagram of the DTI-Alps, EPVS and CPV methodology. (**A**) Schematic diagram of the DTI-ALPS methodology. On the left, place ROIs on the association fibers and projection fibers in bilateral hemispheres. On the right, the spatial relationships among the perivascular space, subcortical fibers (red; x-axis), association fibers (green; y-axis), and projection fibers (blue; z-axis). (**B**) Examples of EPVS on T2-weighted and T2-FLAIR brain MRI scans. i, iv: EPVS in basal ganglia indicated by arrows. ii, v: EPVS in centrum semiovale indicated by arrows. iii, vi: EPVS in midbrain on axial MRI slices indicated by arrows. Scale bar = 10 mm. (**C**) Schematic diagram of the CPV segmented from high-resolution T1-weighted MRI images. Right CPV (red), left CPV (green).
Abbreviations: DTI-ALPS, diffusion tensor image analysis along the perivascular space; EPVS, enlargement perivascular space; CPV, choroid plexus volume; ROIs, regions of interest.

where Dx,proj and Dx,assoc represent the x-axis diffusivities in the projection and association fiber regions, aligned with the perivascular space, and Dy,proj and Dz,assoc are the y-axis and z-axis diffusivities in these regions, orthogonal to the perivascular space.

Quantification of EPVS

EPVS were defined as fluid-filled spaces following the course of penetrating vessels, with a diameter >3 mm, and exhibiting signal intensity similar to that of CSF on all MRI sequences.[32] EPVS number was rated using a validated visual rating scale. Specifically, EPVS in the basal ganglia and centrum semiovale were rated as 0 (0), 1 (1–10), 2 (11–20), 3 (21–40), and 4 (>40),[33,34] EPVS in the midbrain were rated as 0 (not visible) or 1 (visible),as shown in Figure 1B. All assessments were performed by two radiologists (each with over 5 years of experience) who were blinded to clinical data. They received coordinated training using a pilot set of images to ensure consistent application of the rating criteria prior to formal rating.

CPV Segmentation

First, the MRIcroGL (version 20-July-2022) (NITRC: MRIcroGL: Tool/Resource Info) was used to transform the 3D sagittal MPRAGE sequence images of the raw data into 3D NIfTI format files, and then the files were used for total intracranial volume (TIV) calculations and automated segmentation of the left (CPV_l) and right (CPV_r) CP volumes within the lateral ventricles.[35] This was achieved by using Freesurfer 7.4.1 (https://surfer.nmr. mgh.harvard.edu/). The segmentation results were then thoroughly examined by the naked eye by 1 radiologist (with more than 5 years of experience) who was unaware of the clinical information, and manual corrections were made when necessary for the final extraction of the CP volume, which was accomplished through the ITK-SNAP (Version3.8) (http://itksnap.org), as shown in Figure 1C.

Statistical Analysis

SPSS Statistics (version 26, IBM Corporation, Armonk, NY, USA) and GraphPad Prism (version 9, GraphPad Software, San Diego, CA, USA) were used for statistical analysis. Normally distributed variables were expressed as mean±standard deviation, while non-normal data were expressed as median (inter-quartile range, IQR). The inter-observer correlation coefficient (ICC) was used to evaluate radiologists' inter-observer agreement on the DTI-ALPS and EPVS data. Group comparisons were conducted

separately for two-group (PD vs HC) and three-group (PD-A, PD-NA, and HC) analyses using chi-square tests, nonparametric tests, one-way ANOVA or Kruskal–Wallis *H*-tests, as appropriate. For imaging features, analysis of covariance (ANCOVA) was applied to control for age, gender, and education level. If the assumptions of ANCOVA were not met, nonparametric tests were used. Bonferroni and Tukey correction were used for post-hoc comparisons. Furthermore, receiver operating curve (ROC)is was employed to evaluate the diagnostic performance of individual and combined imaging indices in discriminating PD from HC, and to assess the predictive value of imaging indices for anxiety in Parkinson's disease. The optimal cut-off value was determined by maximizing Youden's index (sensitivity + specificity – 1). Area under the curve (AUC) with 95% confidence intervals was reported. Partial correlation analysis was performed to examine the relationship between imaging indices and clinical scores, controlling for age, gender, and education. To account for multiple comparisons, false discovery rate (FDR) correction was applied to significant correlations. A two-tailed P-value < 0.05 was considered statistically significant.

Results

Participant Demographic and Clinical Characteristics

Detailed demographic and clinical characteristics of all PD and HC participants are presented in Table 1 and Supplementary Table S1. There were no significant differences in age (P =0.07), gender (P =0.531), education (P =0.079), or BMI (P =0.607) among the three groups (PD-A, PD-NA, and HC). Compared to HC, the whole PD group showed higher HAM-A (P <0.001), Somatic factors (P <0.001), Psychological factors (P <0.001), HAM-D score (P <0.001), and lower MoCA score (P <0.001). Furthermore, the PD-A group had higher UPDRS I (P =0.013), HAM-A (P

Table 1 Demographic and Clinical Characteristics of the Participants

	PD whole (n=64)	PD-A (n=34)	PD-NA (n=30)	HC (n=42)	$P^{\#}$ value	*P* value
Age (year)	61 (54.3,69.0)	61 (54.8,71.0)	61 (51.5,67.5)	56 (53.0,63.0)	0.07	0.172
Sex,male (%)	43.75	44.12	43.33	35.71	0.531	0.82
Education						
Illiterate	12.28	16.67	7.41	12.5	0.079	0.142
Primary school	31.58	30.00	33.33	12.5		
Middle school	49.12	50.00	48.15	54.17		
College	7.02	3.33	11.11	20.83		
BMI	22.36±3.18	22.36±3.49	22.35±2.83	22.77±3.17	0.607	0.877
Disease duration (years)	3 (1.0,4.0)	3 (1.5,4.0)	3 (1.0,4.3)	-	-	0.56
Onset-age	58(51.0,66.5)	57.58±10.73	58.79±9.86		-	0.651
UPDRS I	4 (2,5)	4 (3,6)	3 (2,4)	-	-	0.013*[a]
UPDRS II	15 (12,19)	16.03±6.08	15.57±4.78	-	-	0.749
UPDRS III	26 (21,36)	26 (21,38)	25.5 (19.3,35.8)	-	-	0.382
UPDRS total	45 (34,60)	49 (39,63.5)	42 (31,58.5)	-	-	0.083
H&Y stage	2 (2,3)	2 (1.5,3.0)	2 (2,3)	-	-	0.514
LEDD (mg)	300 (300,400)	300 (300,400)	300 (300,400)	-	-	0.559
Hcy	12.50 (9.4,13.8)	12.15 (9.6,14)	12.60 (9,14.1)	-	-	0.725
HAM-A	15 (11,17.3)	17 (16,20)	11 (9,13)	6 (5,8)	<0.001***	<0.001***[a,b,c]
Somatic factors	6 (5,8)	8 (6.3,9)	5 (4,6)	3 (3,4)	<0.001***	<0.001***[a,b,c]
Psychological factors	8 (6,12)	12 (9,13)	6 (4.3,8)	3 (2,4)	<0.001***	<0.001***[a,b,c]
HAM-D	15 (10.3,17.8)	16 (14.3,20.8)	11 (8,14.8)	5 (4,7)	<0.001***	<0.001***[a,b,c]
MoCA	17 (14.3,20.0)	18 (14.3,19.8)	16 (14.3,20.8)	23 (21,24.3)	<0.001***	<0.05*[b,c]
PDQ-39	41 (28,50)	42 (30,57)	37.5 (26.3,46)	-	-	0.164
NMSS	35 (26.3,45.5)	43 (29,49.8)	30 (25.3,36.5)	-	-	0.001**[a]

Notes: Results are expressed as means ± standard deviation for the continuous variables and as frequency for the categorical variables.*$P < 0.05$; ** $P < 0.01$; ***$P < 0.001$.[#]indicates *P* between PD whole and HC.[a]indicates *P* between PD-A and PD-NA in post hoc analysis.[b]indicates *P* between PD-A and HC in post hoc analysis.[C]indicates *P* between PD-NA and HC in post hoc analysis.Post hoc multiple comparisons were corrected using the Bonferroni method.
Abbreviations: PD,Parkinson's disease; PD-A, PD patients with anxiety; PD-NA, PD patients without anxiety; HC, healthy control; BMI, body mass index; UPDRS, unified Parkinson's disease rating scale; H&Y stage, Hoehn & Yahr stage; LEDD, levodopa equivalent daily dose; Hcy, Homocysteine; HAM-A, Hamilton anxiety rating scale; HAM-D, Hamilton depression rating scale; MoCA, Montreal Cognitive Assessment; PDQ-39, Parkinson's disease Questionnaire-39; NMSS, Non-Motor Symptom Scale.

<0.001), HAM-D (P <0.001) and NMSS (P =0.001) scores than PD-NA group, post-hoc analyses using both the Bonferroni and Tukey HSD tests confirmed that these differences remained statistically significant (P <0.05).

Inter-Observer Correlation Coefficient(ICC)

Inter-observer agreement was excellent for the DTI-ALPS index (ICC for DTI-ALPS$_l$, 0.83 [95% CI 0.69,0.90]; ICC for DTI-ALPS$_r$, 0.74 [95% CI 0.52,0.85]; ICC for DTI-ALPS$_b$, 0.98 [95% CI 0.69,0.99]). Similarly, EPVS number also demonstrated good inter-observer agreement (ICC for EPVS BG$_l$ number, 0.83 [95% CI 0.79,0.93]; ICC for EPVS BG$_r$ number, 0.93 [95% CI 0.88,0.96]; ICC for EPVS CSO$_l$ number, 0.93 [95% CI 0.88,0.96]; ICC for EPVS CSO$_r$ number, 0.96 [95% CI 0.93,0.97]; ICC for EPVS MB number, 0.88 [95% CI 0.79, 0.94]).

MRI Characteristics in Whole PD and HC Groups

The MRI characteristics of whole PD and HC participants are summarized in Table 2. Compared to HC group, DTI-ALPS$_l$, DTI-ALPS$_r$ and DTI-ALPS$_b$ were significantly lower (all P <0.001), EPVS BG$_l$ number (P <0.001), EPVS BG$_r$ number (P <0.001), EPVS CSO$_l$ number (P =0.048), EPVS MB number (P =0.014), CPV (P =0.023), CPV$_l$ (P =0.017) and CPV$_r$ (P =0.035) were significantly higher in the PD group.

Based on ROC curve analysis, four combined models were compared for their ability to differentiate PD from HC, the AUC for the four models were as follows: 0.827 for the Left-sided Dominance model, 0.789 for the Right-sided Dominance model, 0.828 for the Bilateral Integration model, and 0.847 for the Top Single-Markers model. The Top Single-Markers model, combining DTI-ALPS$_l$, EPVS BG$_r$ number, and CPV$_l$, demonstrated the best discriminatory performance (AUC = 0.847, 95% CI: 0.764–0.931; P <0.001). The optimal cut-off point for this model was 0.712, corresponding to a Youden's index of 0.591, with a sensitivity of 59.1% and a specificity of 100%. Individually, DTI-ALPS$_l$, EPVS BG$_r$ number, and CPV$_l$ had AUCs of 0.774, 0.7, and 0.658. Therefore, the Top Single-Markers combined model demonstrated superior performance in differentiating PD from HC compared to any single imaging biomarker or other combined models, as presented in Table 3, Supplementary Table S2 and Figure 2.

Table 2 MRI Features in Whole PD and HC Participants

	PD whole (n=64)	HC (n=42)	*P* value
DTI-ALPS$_l$	1.540 (1.4,1.7)	1.704 (1.6,1.9)	<0.001***
DTI-ALPS$_r$	1.525 (1.4,1.7)	1.690 (1.5,1.9)	<0.001***
DTI-ALPS$_b$	1.552 (1.4,1.6)	1.748 (1.6,1.9)	<0.001***
EPVS BG$_l$ number	6.000 (4.0,8.0)	3.000 (1.3,4.0)	<0.001***
EPVS BG$_r$ number	7.000 (5.0,9.0)	4.000 (2.3,5.8)	<0.001***
EPVS CSO$_l$ number	6.000 (3.0,10.8)	3.000 (1.0,8.8)	0.048*
EPVS CSO$_r$ number	7.000 (3.0,10.0)	4.000 (1.0,11.0)	0.117
EPVS MB number	1.000 (0.0,2.0)	0.000 (0.0,2.0)	0.014*
TIV(mL)	1444.46 (1327.29,1579.76)	1393.14 (1320.39,1456.46)	0.088
CPV(mL)	1.58 (1.21,1.92)	1.29 (1.09,1.58)	0.023*
CPV,ratio of TIVx10^3	1.06 (0.9,1.2)	0.88 (0.8,1.2)	0.051
CPV$_l$	0.81 (0.64,1.01)	0.64 (0.49,0.82)	0.017*
CPV$_l$, ratio of TIVx10^3	0.54 (0.4,0.6)	0.43 (0.3,0.6)	0.058
CPV$_r$	0.75 (0.59,0.94)	0.64 (0.53,0.76)	0.035*
CPV$_r$,ratio of TIVx10^3	0.51 (0.4,0.6)	0.46 (0.4,0.6)	0.134

Notes: Results are expressed as means ± standard deviation for the continuous variables and as frequency for the categorical variables.*P < 0.05; ***P < 0.001.

Abbreviations: PD, Parkinson's disease; HC, healthy control; DTI-ALPS, diffusion tensor image analysis along the perivascular space; EPVS, enlargement perivascular space; BG, basal ganglia; CSO, centrum semiovale; MB, midbrain; TIV, total intracranial volume; CPV, choroid plexus volume; $_r$, right-hemispheric; $_l$, left-hemispheric; $_b$, bilateral-hemispheric.

Table 3 ROC Analyses of Glymphatic Function Index in PD and HC

Top Single-Markers	AUC	*P*	95% CI	Youden's Index	Sensitivity	Specificity	Cut-off point
DTI-ALPS$_l$	0.774	<0.001***	0.671 ~ 0.877	0.485	0.636	0.848	0.676
EPVS BG$_r$ number	0.7	0.003**	0.580 ~ 0.821	0.318	0.591	0.727	5
CPV$_l$	0.658	0.018*	0.537 ~ 0.780	0.326	0.568	0.758	0.789
Composite model	0.847	<0.001***	0.764 ~ 0.931	0.591	0.591	1	0.721

Notes: *$P < 0.05$; ** $P < 0.01$; ***$P < 0.001$.
Abbreviations: ROC, receiver operating curve; AUC, area under the curve; CI, confidence interval; DTI-ALPS$_l$ left-hemispheric diffusion tensor image analysis along the perivascular space, EPVS BG$_r$ number right-hemispheric basal ganglia enlargement perivascular space number; CPV$_l$, left-hemispheric choroid plexus volume.

MRI Characteristics in PD-A,PD-NA and HC Groups

MRI characteristics of PD-A, PD-NA and HC participants are shown in Table 4, Supplementary Table S1, and Figure 3A–E. In the subgroup analysis of PD, compared to the PD-NA group, the DTI-ALPS$_r$ (P =0.047, Cohen's d= −0.655) and DTI-ALPS$_b$ (P =0.010) were significantly lower in the PD-A group, while the CPV$_l$ was larger (Tukey's HSD, P =0.046). In addition, compared to the HC group, the DTI-ALPS$_l$ (P <0.001), DTI-ALPS$_r$ (P =0.001) and DTI-ALPS$_b$ (P <0.001)were significantly lower, EPVS BG$_l$ number (P <0.001), EPVS BG$_r$ number (P <0.001), EPVS CSO$_l$ number (P =0.005) and EPVS MB number (P =0.003) were significantly higher, as well as CPV (P =0.045, Cohen's d=0.782), CPV$_l$ (P =0.018) were significantly larger in the PD-A group. Besides, compared to the HC group, the DTI-ALPS$_l$ (P =0.045, Cohen's d= −0.698) was significantly lower, EPVS BG$_l$ number (P <0.001), EPVS BG$_r$ number (P <0.001), EPVS CSO$_l$ number (P =0.001) and EPVS MB number (P =0.016) were significantly higher in the PD-NA group, post-hoc analyses using both the Bonferroni and Tukey HSD tests confirmed that these differences remained statistically significant (P <0.05).

Given the significant differences in DTI-ALPS$_b$ and CPV$_l$ between PD-A and PD-NA groups, the predictive efficacy of each indicator alone was first evaluated.DTI-ALPS$_b$ alone predicted anxiety with an AUC of 0.719 (95% CI: 0.563 ~ 0.874), while CPV$_l$ alone achieved an AUC of 0.679 (95% CI: 0.514 ~ 0.843). Subsequently, these two indicators were included in a composite model. The model demonstrated superior predictive efficacy for anxiety in PD patients compared to any single indicator (AUC = 0.748, 95% CI: 0.600–0.895) (Figure 3F). The optimal cut-off point was 0.616, yielding a Youden's index of 0.402, with a sensitivity of 71.4% and a specificity of 68.8%.

Correlation Analysis Among DTI-ALPS Index, EPVS Number and CPV

The DTI-ALPS$_b$ was negatively correlated with the CPV$_l$ (r= −0.338, P=0.025) and CPV (r= −0.354, P=0.018) (Figure 4A and B), according to the correlation analysis of three imaging indices in all PD patients.The rest imaging indices did not show statistically significant correlation.

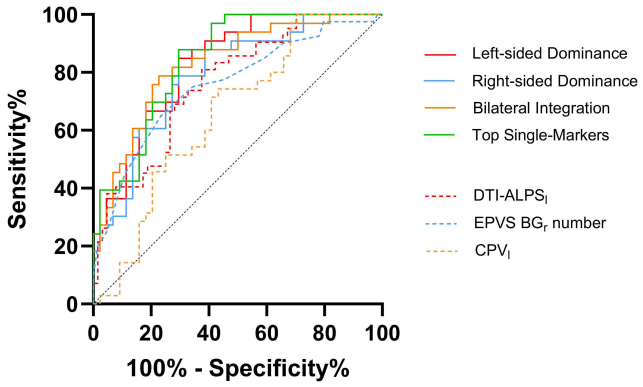

Figure 2 ROC curves for diagnosing PD and HC using single biomarker and composite models.
Abbreviations: PD, Parkinson Disease; HC, healthy control; DTI-ALPS, diffusion tensor image analysis along the perivascular space; EPVS, enlargement perivascular space; BG, basal ganglia; CPV, choroid plexus volume; $_l$, left-hemispheric; $_r$, right-hemispheric; ROC, receiver operating curve.

https://doi.org/10.2147/NDT.S568398

Table 4 MRI Features in PD-A, PD-NA and HC Participants

	PD-A (n=34)	PD-NA (n=30)	HC (n=42)	*P* value	Post hoc tests *P* value		
					PD-A vs HC	PD-NA vs HC	PD-A vs PD-NA
DTI-ALPS$_l$	1.507 (1.3,1.6)	1.562 (1.5,1.7)	1.704 (1.6,1.9)	<0.001***	<0.001***	0.045*	0.062
DTI-ALPS$_r$	1.475 (1.4,1.6)	1.555 (1.5,1.8)	1.690 (1.5,1.9)	0.001**	0.001**	0.439	0.047*
DTI-ALPS$_b$	1.483 (1.4,1.6)	1.573 (1.5,1.8)	1.748 (1.6,1.9)	<0.001***	<0.001***	0.066	0.010*
EPVS BG$_l$ number	5.5 (4.0,7.0)	6(4.8,8.3)	3(1.3,4.0)	<0.001***	<0.001***	<0.001***	1
EPVS BG$_r$ number	7(4.8,9.0)	7(4.8,9.5)	4(2.3,5.8)	<0.001***	<0.001***	<0.001***	1
EPVS CSO$_l$ number	5.5 (2.8,11.3)	6.5 (3.0,10.5)	3(1.0,8.8)	<0.001***	0.005**	0.001**	1
EPVS CSO$_r$ number	6.5 (2.8,11.3)	7.5 (3.8,10.0)	4.(1.0,11.0)	0.063			
EPVS MB number	1(0.0,2.3)	1(0.0,2.0)	0(0.0,2.0)	<0.001***	0.003**	0.016*	1
TIV(mL)	1483.00 (1328.16,1579.76)	1404.05 (1327.29,1608.40)	1393.14 (1320.39,1456.46)	0.353			
CPV(mL)	1.63 (1.39,2.0)	1.41 (1.00,1.60)	1.29 (1.09,1.58)	0.008**	0.045*	1	0.076
CPV,ratio of TIVx10^3	1.16±0.36	0.95±0.31	0.95±0.25	0.081			
CPV$_l$	0.84 (0.67,1.02)	0.68 (0.47,0.83)	0.64 (0.49,0.82)	0.007**	0.018*	1	0.054
CPV$_l$ ratio of TIVx10^3	0.59±0.19	0.48±0.16	0.47±0.15	0.051			
CPV$_r$	0.79 (0.65,0.95)	0.66 (0.53,0.79)	0.64 (0.53,0.76)	0.063			
CPV$_r$,ratio of TIVx10^3	0.56±0.18	0.48±0.16	0.47±0.11	0.162			

Notes: Results are expressed as means ± standard deviation for the continuous variables and as frequency for the categorical variables.*$P < 0.05$; ** $P < 0.01$; ***$P < 0.001$. Post hoc multiple comparisons were corrected using the Bonferroni method.

Abbreviations: PD-A, PD patients with anxiety; PD-NA, PD patients without anxiety; HC, healthy control; DTI-ALPS, diffusion tensor image analysis along the perivascular space; EPVS, enlargement perivascular space; BG, basal ganglia; CSO, centrum semiovale; MB, midbrain; TIV, total intracranial volume; CPV, choroid plexus volume; $_r$, right-hemispheric; $_l$, left-hemispheric; $_b$, bilateral-hemispheric.

Partial Correlation Analysis Between Clinical Features and MRI Features in PD-A Patients

After controlling age, gender and education level, the partial correlation analysis between imaging indices and clinical features in PD-A group was shown in Figure 5. Overall CPV was positively correlated with HAM-A (r =0.657, FDR-corrected P =0.031), Psychological factors (r =0.677, FDR-corrected P =0.025), NMSS (r =0.617, FDR-corrected P =0.041) and Hcy (r =0.611, FDR-corrected P =0.043). CPV, ratio of TIVx10^3 was negatively correlated with MoCA (r = −0.640, FDR-corrected P =0.034), and positively correlated with UPDRS III (r =0.659, FDR-corrected P =0.03) and UPDRS total (r =0.626, FDR-corrected P =0.039). CPV$_l$ was positively correlated with Psychological factors (r =0.719, FDR-corrected P =0.014). CPV$_l$, ratio of TIVx10^3 was positively correlated with UPDRS III (r =0.655, FDR-corrected P =0.029) and UPDRS total (r =0.605, FDR-corrected P =0.044). CPV$_r$ was positively correlated with HAM-A (r =0.683, FDR-corrected P =0.022), Psychological factors (r =0.604, FDR-corrected P =0.043), NMSS (r =0.639, FDR-corrected P =0.033) and Hcy (r =0.608, FDR-corrected P =0.042). CPV$_r$, ratio of TIVx10^3 was negatively correlated with MoCA (r = −0.664, FDR-corrected P =0.028), positively correlated with UPDRS III (r =0.636, FDR-corrected P =0.035) and UPDRS total (r =0.619, FDR-corrected P =0.040). Besides, EPVS BG$_r$ number was positively correlated with HAM-A (r =0.631, FDR-corrected P =0.037), Psychological factors (r =0.695, FDR-corrected P =0.018) and UPDRS I (r =0.609, FDR-corrected P =0.044). (r= 0.527, P=0.044).

Discussion

In this study, we combined DTI-ALPS index, EPVS number and CPV to noninvasively evaluate the brain glymphatic function of PD patients indirectly. The main findings are as follows: (1) PD patients had glymphatic dysfunction, and those with anxiety had more severe damage. (2) The increase of CPV was related to anxiety, cognitive decline and dyskinesia in PD patients with anxiety.

Our study combined three imaging indicators to explore the changes of brain glymphatic system function in PD patients.The observed differences in all three glymphatic imaging metrics between PD patients and HC suggest impaired glymphatic system function in PD, which aligns with previous literature.[36] Additionally, the maximum diagnostic

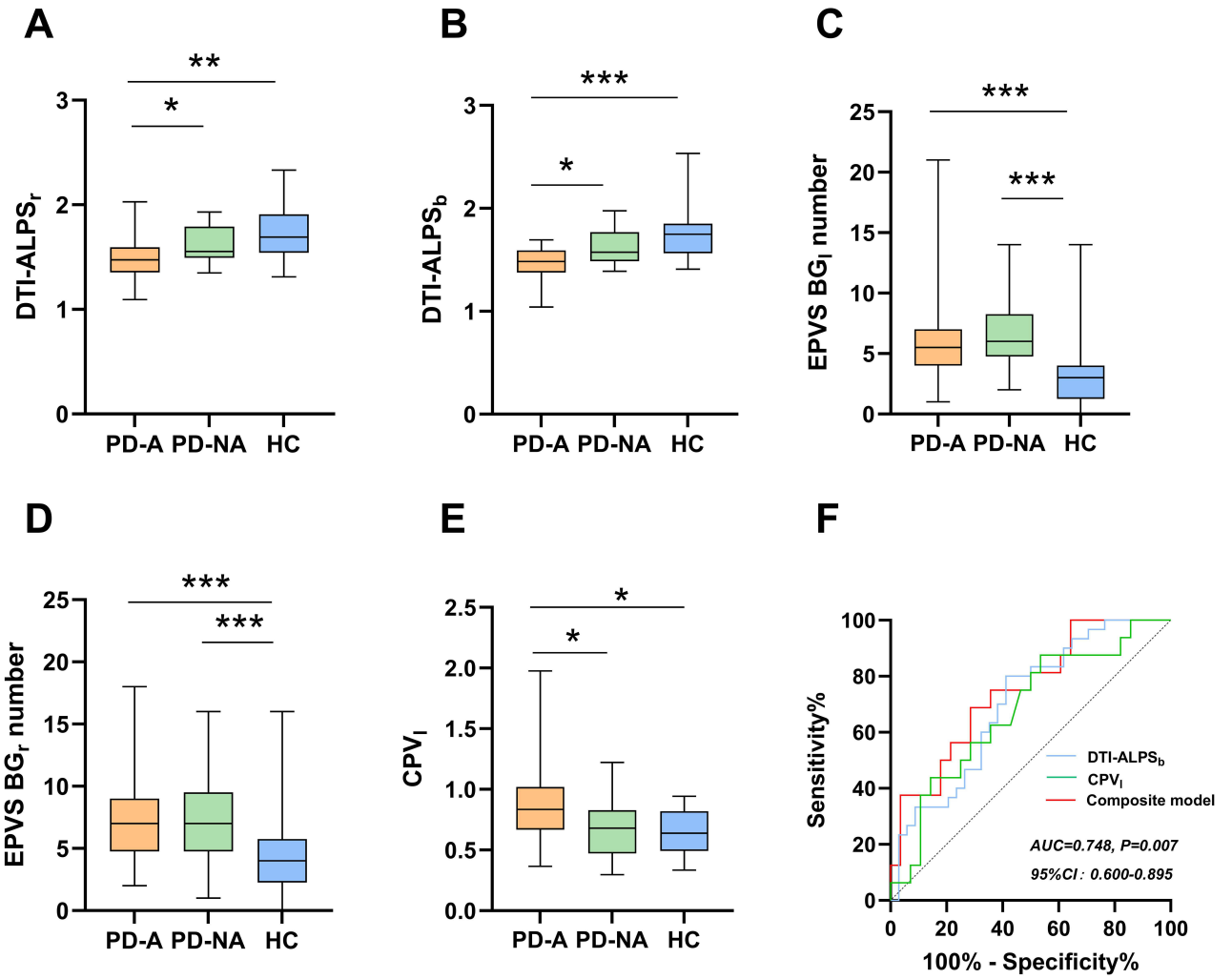

Figure 3 Comparisons of three imaging indicators among the PD-A, PD-NA and HC groups using box plots.Sample sizes: PD-A group (n = 34), PD-NA group (n = 30), HC group (n =42).Group differences for (**A**)–(**E**) were tested using analysis of covariance (ANCOVA) followed by Bonferroni and Tukey's post-hoc test. (**A**) Comparisons of DTI-ALPS$_r$ among the PD-A, PD-NA and HC groups. (**B**) Comparisons of DTI-ALPS$_b$ among the PD-A, PD-NA and HC groups. (**C**) Comparisons of EPVS BG$_l$ number among the PD-A, PD-NA and HC groups. (**D**) Comparisons of EPVS BG$_r$ number among the PD-A, PD-NA and HC groups. (**E**) Comparisons of CPV$_l$ among the PD-A, PD-NA and HC groups.(**F**) ROC curve was used to evaluate the diagnostic accuracy of the DTI-ALPS$_b$, CPV$_l$ and composite model to discriminate PD patients with and without anxiety.

Abbreviations: PD-A, PD patients with anxiety; PD-NA, PD patients without anxiety; HC, healthy control; DTI-ALPS, diffusion tensor image analysis along the perivascular space; EPVS, enlargement perivascular space; BG, basal ganglia; CPV, choroid plexus volume; $_r$, right-hemispheric; $_l$, left-hemispheric; $_b$, bilateral-hemispheric; ROC, receiver operating curve; AUC, area under the ROC curve. *P < 0.05; **P < 0.01; ***P < 0.001.

efficiency for differentiating between PD and HC occurs when the three imaging indicators are combined. At present, the clinical diagnosis of PD mainly depends on clinical manifestations, with imaging contributing relatively little to auxiliary diagnosis, making accurate diagnosis challenging. Therefore, the combined imaging model developed in this study may may serve as a valuable tool to aid in the clinical diagnosis of PD.

In contrast to previous research, our study focused on PD patients with anxiety,we discovered that the PD-A group had a significantly lower DTI-ALPS index and a larger CPV compared to the PD-NA group, suggesting that PD patients with anxiety may have more pronounced glymphatic system impairment. Anxiety may aggravate the dysfunction of brain glymphatic system in patients with Parkinson 's disease. In particular, it could happen in the following ways: First, anxiety is frequently accompanied by increased sympathetic nerve activity and decreased parasympathetic nerve activity, resulting in decreased heart rate variability, vasoconstriction, and reduced cerebral blood flow, which in turn affects the flow of cerebrospinal fluid driven by arterial pulsation and weakens glymphatic clearance function.[37] Secondly, some patients with anxiety may be accompanied by sleep disorders, and the glymphatic system is mainly active during deep

https://doi.org/10.2147/NDT.S568398

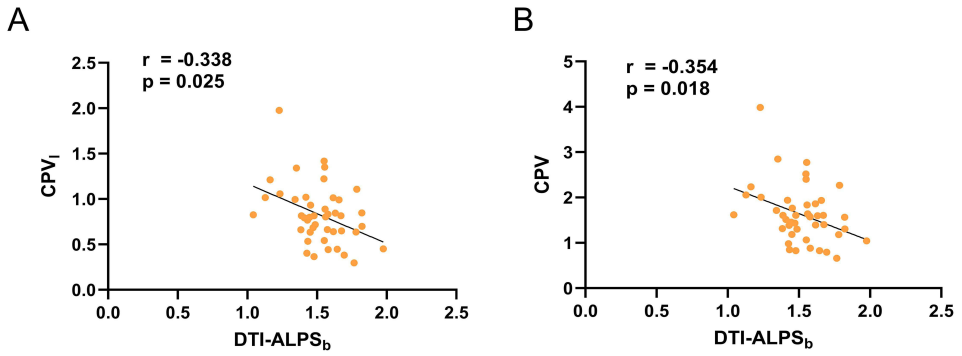

Figure 4 Correlations between DTI-ALPS$_b$ and CPV$_l$, CPV in PD patients. (**A**) Negative correlations between DTI-ALPS$_b$ and CPV$_l$ (r = −0.338, p = 0.025). (**B**) Negative correlations between DTI-ALPS$_b$ and CPV (r = −0.354, p = 0.018).
Abbreviations: PD, Parkinson's disease; DTI-ALPS, diffusion tensor image analysis along the perivascular space; CPV, choroid plexus volume; $_b$, bilateral-hemispheric; $_l$, left-hemispheric.

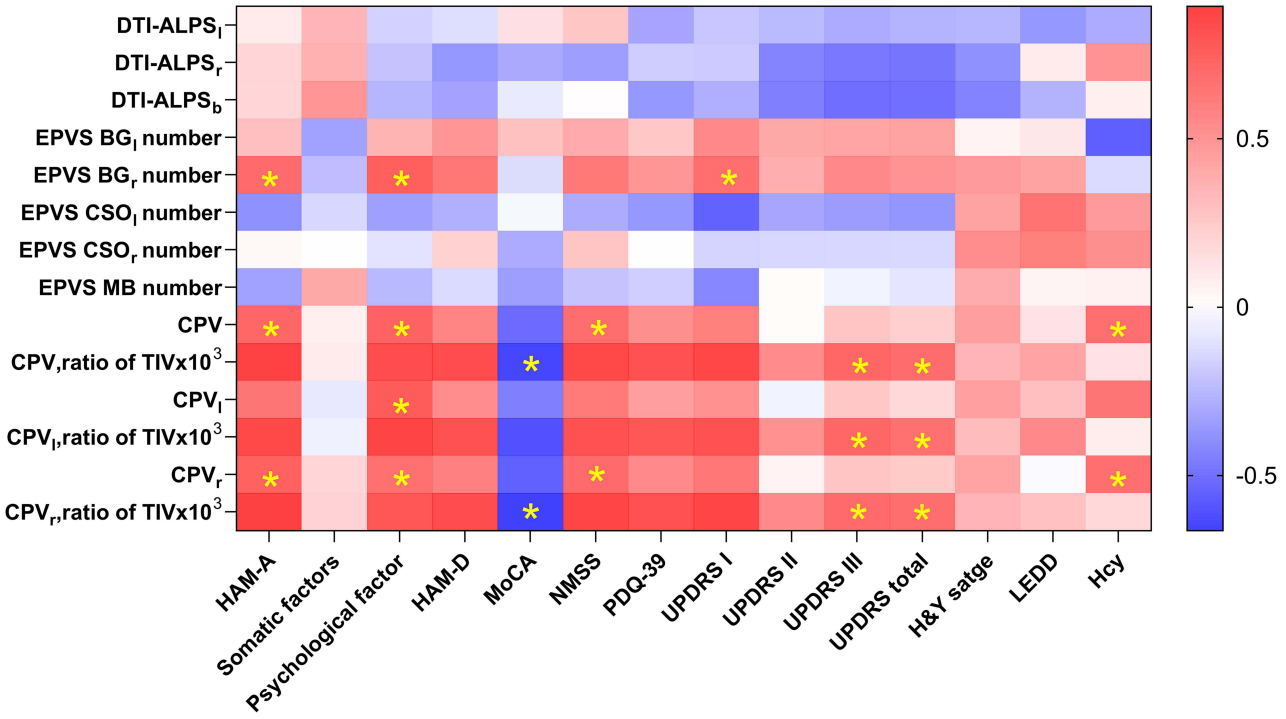

Figure 5 Partial correlation analysis between clinical features and MRI features in PD-A using matrix graph. The color intensity represents the magnitude of the partial correlation coefficient (r), with red indicating positive correlations and blue indicating negative correlations. *P < 0.05.
Abbreviations: DTI-Alps, diffusion tensor image analysis along the perivascular space; EPVS, enlargement perivascular space; BG, basal ganglia; CSO, centrum semiovale; MB, midbrain; TIV, total intracranial volume; CPV, choroid plexus volume; r, right-hemispheric; l, left-hemispheric; b, bilateral-hemispheric; HAM-A, Hamilton anxiety rating scale; HAM-D, Hamilton depression rating scale; MoCA, Montreal Cognitive Assessment; NMSS, Non-Motor Symptom Scale; PDQ-39, Parkinson's disease Questionnaire-39; UPDRS, unified Parkinson's disease rating scale; H&Y stage, Hoehn & Yahr stage; LEDD, levodopa equivalent daily dose; Hcy, Homocysteine.

sleep, and the decrease of sleep quality directly leads to the decrease of glymphatic clearance efficiency. In addition, chronic anxiety can activate the Hypothalamic-Pituitary-Adrenal (HPA) axis, increase cortisol levels, promote neuroinflammation and oxidative stress, damage the function of AQP4 aquaporin on astrocytes, and then affect glymphatic flow.[9] Our findings are inconsistent with those of the study by Gui et al,[38] which found no statistically significant variations in imaging parameters within the anxiety subgroup. Potential causes include: First of all, their study included only 16 PD patients with anxiety, which may have resulted in insufficient statistical power. Furthermore, it may be linked to the use of anti-anxiety and depression medications in the included patients. While PD glymphatic dysfunction has been

demonstrated, there are limited investigations on anxiety subtypes. The findings of previous research differ. Our study provides new insights into the association between PD anxiety subtypes and brain glymphatic system. Nevertheless, in the future, multi-center and large-sample studies are still needed to further confirm the impact of PD neuropsychiatric symptoms on the glymphatic system.

Curiously, subgroup analysis did not reveal a significantly higher number of EPVS in the PD-A group compared to the PD-NA group, as initially anticipated. This discrepancy may be attributed to the following reasons: on the one hand, the mechanism of PVS enlargement is related to advanced age, hypertensive biomarkers, and arterial stiffness severity.[39,40] When we included PD patients, we excluded patients with hypertension and stroke, and there was no significant difference in age between PD subgroups. On the other hand, the core mechanism of anxiety is the functional connectivity disorder composed of amygdala, prefrontal cortex, anterior cingulate gyrus, hippocampus and insula,[41] which almost does not involve the above three dimensions of PVS number. This finding seems to suggest that anxiety aggravates the brain glymphatic system dysfunction in this study, which is primarily due to functional changes rather than structural ones yet. Consequently, in early stages, the DTI-ALPS index appears more sensitive than EPVS number in capturing functional impairment of the glymphatic system.

This study suggests that PD-A patients have a possible association with altered brain waste clearance as indicated by reduced DTI-ALPS$_r$, DTI-ALPS$_b$. The impairment likely begins in the right hemisphere, because the right side of the brain processes emotions and has high metabolic activity,[42] which may make it more vulnerable under PD background. The observed bilateral reduction may reflect a subsequent progression of dysfunction to involve both hemispheres. In addition, the CPV$_1$ showed a trend toward enlargement. This may be a compensatory response to the reduced waste clearance or could be related to local inflammation in the brain. This is partially consistent with the study of Qin et al.[43] They observed that the right brain glymphatic system was more severely damaged when they explored the relationship between motor symptoms and glymphatic system function in PD patients. In contrast, an earlier study by Shen[44] et al found that glymphatic dysfunction in early PD was more significant in the left hemisphere, with bilateral impairment emerging only in later disease stages, suggesting a left-to-right progression with disease advancement.Therefore, the lateralization of brain glymphatic function damage in PD subtypes is still controversial. In the future, it is necessary to merge multimodal brain network and functional technologies to further investigate.[41]

The DTI-ALPS method has gained increasing attention for its association with pathology and clinical manifestations in recent studies.[45] However, its validity has been questioned as it primarily assesses water molecule diffusion near the lateral ventricles not fully reflect the function of the brain glymphatic system.[46] The CP is a key component of the brain glymphatic system. As the starting point of the CSF circulation, it drives the CSF circulation to construct a circulation pathway of the perivascular space-cerebral parenchyma-perivenous space, regulating ion transport and metabolite clearance.[47] The increase of CPV may widely affect the downstream structure of the glymphatic system. As an upstream structure of the brain glymphatic system, CPV may have the potential to indirectly evaluate the glymphatic system. In our study, the DTI-ALPS index correlated negatively with CPV, suggesting these metrics offer complementary information. This finding aligns with the findings of the Deng[36] et al study. At present, the research on CPV and glymphatic system function is in an emerging stage. Current research on CPV and glymphatic function remains nascent, with prior studies spanning AD,[48] PD,[49] depression,[50] adult hyperactivity disorder (ADHD)[51] and type I narcolepsy,[52] though exploration in PD has been limited mainly to motor function[49] and cognitive correlates.[53] Our research expands PD non-motor symptom research through a new perspective of CPV and glymphatic function. However, CPV enlargement is not only related to the removal of brain metabolic waste, but also to circadian rhythm, immune regulation, aging and other reasons, which should be carefully explained. Beyond CPV, future studies should also focus on the morphological changes of the CP. For instance, Zhen et al observed CP hypertrophy and cystic degeneration (grape sign) in AD and PD on 7.0TMRI,[54] which may be closely related to neurodegenerative changes.

Our analysis revealed significant correlations between CPV and multiple clinical scales in PD patients with anxiety. In particular, increased CPV in PD patients with anxiety was associated with anxiety, cognitive decline, quality of life, and motor impairment. Compared to previous studies, our work emphasizes an association between non-motor symptoms of PD and brain glymphatic function impairment. In terms of anxiety and depression, our findings are consistent with those of Shen44 et al, who showed a negative correlation between PVS burden and HAM-A in patients with PD. However, this

correlation was not found by He et al.[55] This disparity may be attributed to small sample or the usage of psychotropic drug. It also reflects the complexity of the association between mood-related non-motor symptoms and brain glymphatic system, which needs to be further validated by large-sample, multi-center studies in the future. Our results also revealed the correlation between anxiety and motor symptoms, which is similar to the study of Nóbrega-Sousa et al,[56] who noted that walking and obstacle avoidance abilities of PD patients were affected by depression and anxiety symptoms. Therefore, a comprehensive assessment and individualized management of anxiety may not only improve psychiatric outcomes but also potentially ameliorate motor function and enhance the overall quality of life for PD patients and their caregivers relatives.

This study has several limitations. First of all, its cross-sectional, single-center design and modest sample size preclude causal inferences, necessitating future large-scale longitudinal validation. The exclusion of patients with hypertension or diabetes enhances internal homogeneity but may limit generalizability to the broader PD population. Although patients with severe white matter hyperintensities (WMH) were excluded and ROIs were carefully placed to avoid WMH, a potential confounding influence on the DTI-ALPS index cannot be entirely ruled out. Furthermore, the DTI-ALPS index was not normalized for total intracranial volume, which future studies should address to standardize methodology. Moreover, EPVS quantification relied on a visual rating scale across limited brain regions, which, despite excellent inter-observer agreement, remains a subjective measure compared to potential automated methods.[22,36]

Conclusion

In conclusion, our findings indicate that PD patients have cerebral glymphatic dysfunction, with anxiety causing more severe damage. The increase of CPV is related to the increase of anxiety, cognitive decline and dyskinesia in PD patients with anxiety. Overall, multi-parameter glymphatic assessment (including DTI-ALPS, CPV, and EPVS) shows promise as an imaging biomarker for the precision diagnosis of Parkinson's disease.

Data Sharing Statement

The data that support the findings of this study are available from the corresponding author upon reasonable request.

Ethics Approval and Informed Consent

All procedures involving human participants were carried out in accordance with the ethical standards of the institutional and/or national research committee and with the1964 Helsinki Declaration and its later amendments or comparable ethical standards. This article does not contain any experiments with animals.Informed consent was obtained from all individual participants included in the study.

Consent for Publication

The authors affirm that human research participants provided informed consent for publication of the images.

Acknowledgments

We would like to thank the PD patients and healthy controls who spent their time to participate in this study.

Author Contributions

All authors made a significant contribution to the work reported, whether that is in the conception, study design, execution, acquisition of data, analysis and interpretation, or in all these areas; took part in drafting, revising or critically reviewing the article; gave final approval of the version to be published; have agreed on the journal to which the article has been submitted; and agree to be accountable for all aspects of the work.

Funding

This work was supported by the National Natural Science Foundation of China [grant numbers 62376112]; and The Open Project of the Provincial Key Clinical Specialty of Medical Imaging Department of the First People's Hospital of Yunnan Province [2024YXKFKT-05].

Disclosure

The authors declare that they have no known competing financial interests or personal relationships that could have appeared to influence the work reported in this paper.

References

1. Su D, Cui Y, He C, et al. Projections for prevalence of Parkinson's disease and its driving factors in 195 countries and territories to 2050: modelling study of global burden of disease study 2021. *BMJ*. 2025;388:e080952. doi:10.1136/bmj-2024-080952
2. Spillantini MG, Schmidt ML, Lee VM, Trojanowski JQ, Jakes R, Goedert M. Alpha-synuclein in Lewy bodies. *Nature*. 1997;388(6645):839–840. doi:10.1038/42166
3. Bloem BR, Okun MS, Klein C. Parkinson's disease. *Lancet*. 2021;397(10291):2284–2303. doi:10.1016/S0140-6736(21)00218-X
4. Wang H, Zhao Y, Schrag A. Development of anxiety in early Parkinson's disease: a clinical and biomarker study. *Eur J Neurol*. 2023;30(9):2661–2668. doi:10.1111/ene.15890
5. Yao C, Niu L, Fu Y, et al. Cognition, motor symptoms, and glycolipid metabolism in Parkinson's disease with depressive symptoms. *J Neural Transm*. 2022;129(5–6):563–573. doi:10.1007/s00702-021-02437-6
6. Ryu DW, Yoo SW, Choi KE, Oh YS, Kim JS. Correlation of olfactory function factors with cardiac sympathetic denervation in Parkinson's disease. *J Neurol*. 2024;271(3):1397–1407. doi:10.1007/s00415-023-12080-8
7. Poon SF, Tan CH, Hong WP, Chen KC, Yu RL. Tailoring anxiety assessment for Parkinson's disease: the Chinese Parkinson anxiety scale with cultural and situational anxiety considerations. *Soc sci med*. 2025;381:118284. doi:10.1016/j.socscimed.2025.118284
8. Menkü BE, Akın S, Tamdemir SE, Genis B, Altıparmak T, Cosar B. Diagnostic transitions from primary psychiatric disorders to underlying medical conditions: a 5-year retrospective survey from a university hospital sample. *Alpha Psychiatry*. 2024;25(2):226–232. doi:10.5152/alphapsychiatry.2024.231274
9. Khatri DK, Choudhary M, Sood A, Singh SB. Anxiety: an ignored aspect of Parkinson's disease lacking attention. *Biomed Pharmacother*. 2020;131:110776. doi:10.1016/j.biopha.2020.110776
10. Zhang X, Jin Y, Wang M, et al. The impact of anxiety on gait impairments in Parkinson's disease: insights from sensor-based gait analysis. *J Neuroeng Rehabil*. 2024;21(1):68. doi:10.1186/s12984-024-01364-3
11. Iliff JJ, Wang M, Liao Y, et al. A paravascular pathway facilitates CSF flow through the brain parenchyma and the clearance of interstitial solutes, including amyloid β. *Sci Transl Med*. 2012;4(147):147ra111. doi:10.1126/scitranslmed.3003748
12. Rasmussen MK, Mestre H, Nedergaard M. The glymphatic pathway in neurological disorders. *Lancet Neurol*. 2018;17(11):1016–1024. doi:10.1016/S1474-4422(18)30318-1
13. Aspelund A, Antila S, Proulx ST, et al. A dural lymphatic vascular system that drains brain interstitial fluid and macromolecules. *J Exp Med*. 2015;212(7):991–999. doi:10.1084/jem.20142290
14. Da Mesquita S, Louveau A, Vaccari A, et al. Functional aspects of meningeal lymphatics in ageing and Alzheimer's disease. *Nature*. 2018;560(7717):185–191. doi:10.1038/s41586-018-0368-8
15. Zhang Y, Zhang C, He XZ, et al. Interaction between the glymphatic system and α-synuclein in parkinson's disease. *Mol Neurobiol*. 2023;60(4):2209–2222. doi:10.1007/s12035-023-03212-2
16. Boland B, Yu WH, Corti O, et al. Promoting the clearance of neurotoxic proteins in neurodegenerative disorders of ageing. *Nat Rev Drug Discov*. 2018;17(9):660–688. doi:10.1038/nrd.2018.109
17. Taoka T, Masutani Y, Kawai H, et al. Evaluation of glymphatic system activity with the diffusion MR technique: diffusion tensor image analysis along the perivascular space (DTI-Alps) in Alzheimer's disease cases. *Jpn J Radiol*. 2017;35(4):172–178. doi:10.1007/s11604-017-0617-z
18. Taoka T, Ito R, Nakamichi R, et al. Reproducibility of diffusion tensor image analysis along the perivascular space (DTI-Alps) for evaluating interstitial fluid diffusivity and glymphatic function: cHanges in Alps index on Multiple conditiON acquIsition eXperiment (CHAMONIX) study. *Jpn J Radiol*. 2022;40(2):147–158. doi:10.1007/s11604-021-01187-5
19. Hsu JL, Wei YC, Toh CH, et al. Magnetic resonance images implicate that glymphatic alterations mediate cognitive dysfunction in alzheimer disease. *Ann Neurol*. 2023;93(1):164–174. doi:10.1002/ana.26516
20. McKnight CD, Trujillo P, Lopez AM, et al. Diffusion along perivascular spaces reveals evidence supportive of glymphatic function impairment in Parkinson disease. *Parkinsonism Relat Disord*. 2021;89:98–104. doi:10.1016/j.parkreldis.2021.06.004
21. Lee DA, Park BS, Ko J, et al. Glymphatic system dysfunction in temporal lobe epilepsy patients with hippocampal sclerosis. *Epilepsia Open*. 2022;7(2):306–314. doi:10.1002/epi4.12594
22. Shen T, Yue Y, Zhao S, et al. The role of brain perivascular space burden in early-stage Parkinson's disease. *NPJ Parkinsons Dis*. 2021;7:12. doi:10.1038/s41531-021-00155-0
23. Bouvy WH, Zwanenburg JJM, Reinink R, et al. Perivascular spaces on 7 Tesla brain MRI are related to markers of small vessel disease but not to age or cardiovascular risk factors. *J Cereb Blood Flow Metab*. 2016;36(10):1708–1717. doi:10.1177/0271678X16648970
24. Li Y, Zhou Y, Zhong W, et al. Choroid plexus enlargement exacerbates white matter hyperintensity growth through glymphatic impairment. *Ann Neurol*. 2023;94(1):182–195. doi:10.1002/ana.26648
25. Thompson D, Brissette CA, watt JA. The choroid plexus and its role in the pathogenesis of neurological infections. *Fluids Barriers CNS*. 2022;19(1):75. doi:10.1186/s12987-022-00372-6
26. Liu DX, He X, Wu D, et al. Continuous theta burst stimulation facilitates the clearance efficiency of the glymphatic pathway in a mouse model of sleep deprivation. *Neurosci Lett*. 2017;653:189–194. doi:10.1016/j.neulet.2017.05.064
27. Vasciaveo V, Iadarola A, Casile A, et al. Sleep fragmentation affects glymphatic system through the different expression of AQP4 in wild type and 5xFAD mouse models. *Acta Neuropathol Commun*. 2023;11(1):16. doi:10.1186/s40478-022-01498-2
28. Barlattani T, Grandinetti P, Di Cintio A, et al. Glymphatic system and psychiatric disorders: a rapid comprehensive scoping review. *Curr Neuropharmacol*. 2024;22(12):2016–2033. doi:10.2174/1570159X22666240130091235
29. Genel O, Pariante CM, Borsini A. The role of AQP4 in the pathogenesis of depression, and possible related mechanisms. *Brain Behav Immun*. 2021;98:366–377. doi:10.1016/j.bbi.2021.08.232

30. Kim YK, Jeon SW. Neuroinflammation and the immune-kynurenine pathway in anxiety disorders. *Curr Neuropharmacol*. 2018;16(5):574–582. doi:10.2174/1570159X15666170913110426
31. Cohen J. *Statistical Power Analysis for the Behavioral Sciences*. Elsevier Science; 2013.
32. Wardlaw JM, Smith EE, Biessels GJ, et al. Neuroimaging standards for research into small vessel disease and its contribution to ageing and neurodegeneration. *Lancet Neurol*. 2013;12(8):822–838. doi:10.1016/S1474-4422(13)70124-8
33. Potter GM, Chappell FM, Morris Z, Wardlaw JM. Cerebral perivascular spaces visible on magnetic resonance imaging: development of a qualitative rating scale and its observer reliability. *Cerebrovasc Dis*. 2015;39(3–4):224–231. doi:10.1159/000375153
34. Chen H, Wan H, Zhang M, Wardlaw JM, Feng T, Wang Y. Perivascular space in Parkinson's disease: association with CSF amyloid/tau and cognitive decline. *Parkinsonism Related Disord*. 2022;95:70–76. doi:10.1016/j.parkreldis.2022.01.002
35. Fischl B. FreeSurfer. *Neuroimage*. 2012;62(2):774–781. PMID: 22248573; PMCID: PMC3685476. doi:10.1016/j.neuroimage.2012.01.021
36. Deng JH, Zhang HW, Lan XX, et al. Different imaging evaluating performances between glymphatic system and motor symptoms and levodopa responsiveness of parkinson disease. *J Comput Assist Tomogr*. doi:10.1097/RCT.0000000000001720
37. Kiviniemi V, Wang X, Korhonen V, et al. Ultra-fast magnetic resonance encephalography of physiological brain activity – glymphatic pulsation mechanisms? *J Cereb Blood Flow Metab*. 2016;36(6):1033–1045. doi:10.1177/0271678X15622047
38. Gui Q, Meng J, Shen M, et al. Relationship of glymphatic function with cognitive impairment, sleep disorders, anxiety and depression in patients with parkinson's disease. *Neuropsychiatr Dis Treat*. 2024;20:1809. doi:10.2147/NDT.S480183
39. Sibilia F, Sheikh-Bahaei N, Mack WJ, Choupan J. Alzheimer's disease neuroimaging initiative. perivascular spaces in alzheimer's disease are associated with inflammatory, stress-related, and hypertension biomarkers. bioRxiv. doi:10.1101/2023.06.02.543504
40. Bae JH, Kim JM, Park KY, Han SH. Association between arterial stiffness and the presence of cerebral small vessel disease markers. *Brain Behav*. 2021;11(1):e01935. doi:10.1002/brb3.1935
41. Carey G, Görmezoğlu M, de Jong JJA, et al. Neuroimaging of anxiety in parkinson's disease: a systematic review. *Mov Disord*. 2021;36(2):327–339. doi:10.1002/mds.28404
42. Bui T, Neuroanatomy DJM. Cerebral Hemisphere. In: StatPearls. StatPearls Publishing; 2025. Accessed September 13, 2025. http://www.ncbi.nlm.nih.gov/books/NBK549789/.
43. Qin Y, He R, Chen J, et al. Neuroimaging uncovers distinct relationships of glymphatic dysfunction and motor symptoms in Parkinson's disease. *J Neurol*. 2023;270(5):2649–2658. doi:10.1007/s00415-023-11594-5
44. Shen T, Yue Y, Ba F, et al. Diffusion along perivascular spaces as marker for impairment of glymphatic system in Parkinson's disease. *npj Parkinsons Dis*. 2022;8(1):174. doi:10.1038/s41531-022-00437-1
45. Haller S, Moy L, Anzai Y. Evaluation of diffusion tensor imaging analysis along the perivascular space as a marker of the glymphatic system. *Radiology*. 2024;310(1):e232899. doi:10.1148/radiol.232899
46. Ringstad G. Glymphatic imaging: a critical look at the DTI-Alps index. *Neuroradiology*. 2024;66(2):157–160. doi:10.1007/s00234-023-03270-2
47. Municio C, Carrero L, Antequera D, Carro E. Choroid plexus aquaporins in CSF homeostasis and the glymphatic system: their relevance for alzheimer's disease. *Int J Mol Sci*. 2023;24(1):878. doi:10.3390/ijms24010878
48. Choi JD, Moon Y, Kim HJ, Yim Y, Lee S, Moon WJ. Choroid plexus volume and permeability at brain mri within the alzheimer disease clinical spectrum. *Radiology*. 2022;304(3):635–645. doi:10.1148/radiol.212400
49. Jeong SH, Park CJ, Jeong HJ, et al. Association of choroid plexus volume with motor symptoms and dopaminergic degeneration in Parkinson's disease. *J Neurol Neurosurg Psychiatry*. 2023;94(12):1047–1055. doi:10.1136/jnnp-2023-331170
50. Gong W, Zhai Q, Wang Y, et al. Glymphatic function and choroid plexus volume is associated with systemic inflammation and oxidative stress in major depressive disorder. *Brain Behav Immun*. 2025;128:266–275. doi:10.1016/j.bbi.2025.04.008
51. Fang Y, Peng J, Chu T, Gao F, Xiong F, Tu Y. Glymphatic system dysfunction in adult ADHD: relationship to cognitive performance. *J Affect Disord*. 2025;379:150–158. doi:10.1016/j.jad.2025.03.059
52. Hu P, Yuan Y, Zou Y, et al. Alterations in the DTI-Alps index and choroid plexus volume are associated with clinical symptoms in participants with narcolepsy type 1. *Sleep Med*. 2024;124:471–478. doi:10.1016/j.sleep.2024.10.019
53. SH J, HJ J, Sunwoo MK, et al. Association between choroid plexus volume and cognition in Parkinson disease. *Eur J Neurol*. 2023;30(10):3114–3123. doi:10.1111/ene.15999
54. Zhen Z, Zhang R, Gui L, et al. Choroid plexus cysts on 7T MRI: relationship to aging and neurodegenerative diseases. *Alzheimers Dement*. 2024;21(2):e14484. doi:10.1002/alz.14484
55. He P, Shi L, Li Y, et al. The association of the glymphatic function with parkinson's disease symptoms: neuroimaging evidence from longitudinal and cross-sectional studies. *Ann Neurol*. 2023;94(4):672–683. doi:10.1002/ana.26729
56. Nóbrega-Sousa P, Orcioli-Silva D, Lirani-Silva E, Beretta VS, Vitório R, Gobbi LTB. Usual walking and obstacle avoidance are influenced by depressive and anxiety symptoms in patients with Parkinson's disease. *Geriatr Gerontol Int*. 2019;19(9):868–873. doi:10.1111/ggi.13731